NASA/TM – 2024-219027/ Vol. 12

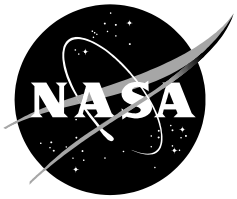

PACE Technical Report Series, Volume 12

Editors:
Ivona Cetinić, GESTAR II/Morgan State University, Baltimore, Maryland
Charles R. McClain, Science Applications International Corporation, McLean, Virginia
P. Jeremy Werdell, NASA Goddard Space Flight Center, Greenbelt, Maryland

The PACE Level 1C data format

Kirk D. Knobelspiesse, NASA Goddard Space Flight Center, Greenbelt, Maryland
Frederick S. Patt, Science Applications International Corporation, Reston, Virginia
Martin A. Montes, Science Systems and Applications Inc., Lanham, Maryland
Sean W. Bailey, NASA Goddard Space Flight Center, Greenbelt, Maryland
Brian Cairns, NASA Goddard Institute for Space Studies, New York, New York
Bryan A. Franz, NASA Goddard Space Flight Center, Greenbelt, Maryland
Meng Gao, Science Systems and Applications Inc., Lanham, Maryland
Andrew M. Sayer, GESTAR II/University of Baltimore County, Baltimore, Maryland

March 2024

NASA STI Program Report Series

The NASA STI Program collects, organizes, provides for archiving, and disseminates NASA's STI. The NASA STI program provides access to the NTRS Registered and its public interface, the NASA Technical Reports Server, thus providing one of the largest collections of aeronautical and space science STI in the world. Results are published in both non-NASA channels and by NASA in the NASA STI Report Series, which includes the following report types:

- TECHNICAL PUBLICATION. Reports of completed research or a major significant phase of research that present the results of NASA Programs and include extensive data or theoretical analysis. Includes compilations of significant scientific and technical data and information deemed to be of continuing reference value. NASA counterpart of peer-reviewed formal professional papers but has less stringent limitations on manuscript length and extent of graphic presentations.

- TECHNICAL MEMORANDUM. Scientific and technical findings that are preliminary or of specialized interest, e.g., quick release reports, working papers, and bibliographies that contain minimal annotation. Does not contain extensive analysis.

- CONTRACTOR REPORT. Scientific and technical findings by NASA-sponsored contractors and grantees.

- CONFERENCE PUBLICATION. Collected papers from scientific and technical conferences, symposia, seminars, or other meetings sponsored or co-sponsored by NASA.

- SPECIAL PUBLICATION. Scientific, technical, or historical information from NASA programs, projects, and missions, often concerned with subjects having substantial public interest.

- TECHNICAL TRANSLATION. English-language translations of foreign scientific and technical material pertinent to NASA's mission.

Specialized services also include organizing and publishing research results, distributing specialized research announcements and feeds, providing information desk and personal search support, and enabling data exchange services.

For more information about the NASA STI program, see the following:

- Access the NASA STI program home page at http://www.sti.nasa.gov

- Help desk contact information:

https://www.sti.nasa.gov/sti-contact-form/ and select the "General" help request type.

NASA/ TM – 2024-219027/ Vol. 12

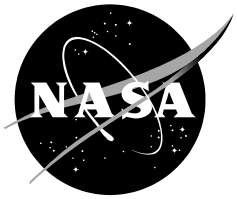

PACE Technical Report Series, Volume 12

Editors:
Ivona Cetinić, GESTAR II/Morgan State University, Baltimore, Maryland
Charles R. McClain, Science Applications International Corporation, McLean, Virginia
P. Jeremy Werdell, NASA Goddard Space Flight Center, Greenbelt, Maryland

The PACE Level 1C data format

Kirk D. Knobelspiesse, NASA Goddard Space Flight Center, Greenbelt, Maryland
Frederick S. Patt, Science Applications International Corporation, Reston, Virginia
Martin A. Montes, Science Systems and Applications Inc., Lanham, Maryland
Sean W. Bailey, NASA Goddard Space Flight Center, Greenbelt, Maryland
Brian Cairns, NASA Goddard Institute for Space Studies, New York, New York
Bryan A. Franz, NASA Goddard Space Flight Center, Greenbelt, Maryland
Meng Gao, Science Systems and Applications Inc., Lanham, Maryland
Andrew M. Sayer, GESTAR II/University of Baltimore County, Baltimore, Maryland

National Aeronautics and
Space Administration

Goddard Space Flight Center
Greenbelt, MD 20771-0001

March 2024

Table of Contents

List of Figures

List of Tables

SUMMARY OF MODIFICATIONS

2024 / 2 / 22

- Numerous updates to how the scattering angle (eqn 1) and rotation angle (eqn 5) are represented. The previous version had a typo in eqn 5, and in fixing that we decided to represent the multiple (yet equivalent) ways to calculate these geometry parameters. Different conventions are used in different fields, but the calculated values are the same, and now this document demonstrates that.

2023 / 10 / 03

- Updated the solar/observation geometry figure (4) to more precisely describe this and the relation to geometry parameters in the file format. Updated the text to correspond with this, and what HARP2 and SPEXone instrument teams are using as geometry conventions.
- Fixed various formatting/font/table presentation problems.

2023 / 09 / 28

- Changed unit to 'degrees' for the *platform_lat* and *platform_lon* fields in the *aircraft_platform* group.
- Noted that filenames for airborne datasets may differ from ocean color conventions, and gave an example convention for the PACE-PAX field campaign.

2023 / 08 / 30

- Added *rotation_angle* field to *geolocation_data* group.
- Renamed *altitude* field to *height*. This makes the description of this field (defining bin location above the ellipsoid) consistent with description in L1B files.
- Modified fields ending in *_noise* to be *_stdev* and updated description text to clarify that this is the standard deviation of values in a bin. Note some descriptions used 'RMSE' which is technically representative of the difference between a model and the data, and thus not appropriate for our purposes.
- Fields in groups are listed as 'name'. No short name is identified. In some cases, what is in the 'description' column is listed in CDLs as a long name, and some effort must be made to coordinate this across data levels and products
- Renamed variables as lower case, to make it clearer they are case insensitive.
- Removed the 'bitwise' quality control flags. The reasoning is that such flags at L1B will be used to select which data are binned at L1C, and are thus unnecessary. A general QC field remains, although the definition of the values is TBD
- Added a section about Airborne Datasets and an optional group *aircraft_platform*. This is intended for airborne remote sensing datasets which are created at L1C for ease in validation efforts. While geolocation strategy may vary, the field names and groups are identical. The additional *aircraft_platform* group provides for relevant information not otherwise contained in the L1C file.
- Updated file naming convention link to: https://oceancolor.gsfc.nasa.gov/resources/docs/filenaming-convention/
- Added description of an L1C grid file, which defines the geolocation grid but does not have observational data

- Added global attributes *geospatial_bounds, geospatial_bounds_crs, geospatial_lat_min, geospatial_lat_max, geospatial_lon_min, geospatial_lon_max* as described in: https://wiki.esipfed.org/Attribute_Convention_for_Data_Discovery_1-3

1 INTRODUCTION

Purpose

NASA's Plankton, Aerosol, Cloud, ocean Ecosystem (PACE) mission will make global ocean color and atmospheric measurements to provide extended data records of ocean ecology and global biogeochemistry, along with polarimetric measurements for advanced observations of aerosols, clouds and the ocean. PACE will contain three instruments: the primary Ocean Color Instrument (OCI), and two multi-angle polarimeters (MAPs). The latter instruments are contributed under a 'Do-No-Harm' (to the rest of the PACE mission) principle, and the PACE Science Data Processing System (SDPS) is only required to produce Level-1b (geolocated radiances with calibration applied) data without performance requirements. However, there is a strong desire to produce data in a format that merges the disparate spatial resolutions, viewing geometry and sampling nature of the three instruments. Our terminology for this format is Level 1c (L1C). This format will be an input to Level 2 algorithms produced from standalone MAP instrument observations, or from algorithms employing multi-sensor fusion.

Creating the L1C format has several components. This includes choice of projection method, the means by which multi-angle views are properly incorporated into that projection ('aggregation') the means to represent wavelength and light polarization state, the selection of data to be included within the L1C file, and the handling of ancillary data either required for L1C file generation or needed in that format for L2 processing.

> The guiding philosophy of the PACE L1C file format is to be a means to gather data from all instruments onto a common sampling grid. This grid will be equal area and contain observations for all instruments and viewing angles for a specified height.

PACE serves the needs of multiple disciplines, and as such there may exist various preferences for L1C format depending on the application. It may not be possible to satisfy all potential users, who may need to re-project or otherwise process L1C data depending on its usage.

The purpose of this document is therefore to describe the L1C file format to be universally applied for PACE, which can be used to produce L2 products.

Instrument Specifics

While detailed descriptions of the three PACE instruments can be found elsewhere (e.g. Werdell et al., 2019, Martins et al., 2018, Hasekamp et al., 2019, among others) we provide a brief description of the spectral, polarimetric and geometric aspects of each instrument in Table 1.

Table 1 Instrument characteristics

	Ocean Color Instrument (OCI)	**Hyper-Angular Rainbow Polarimeter 2 (HARP2)**	**Spectro-Polarimeter for Planetary Exploration one (SPEXone)**
UV-VIS radiance channels	**240**: continuous coverage in 340-890nm range at 2.5nm spectral resolution (5nm bandwidth)	**4**: 441, 549, 669, 873 nm	~**400**: continuous coverage in 385-770nm at 2-5nm spectral resolution

UV-VIS polarimetric channels	-	**4**: 441, 549, 669, 873 nm	~**50**: continuous coverage in 385-770nm at 10-40nm spectral resolution
SWIR radiance channels	**7:** 940, 1038, 1250, 1378, 1615, 2130, and 2260 nm	-	-
Viewing zenith angles in the satellite reference frame for swath center	**1**: 20˚ North in northern hemisphere, 20˚ South in southern hemisphere to avoid ocean surface glint	**60** angles between ± 57˚ along track for 669 nm, **10** angles for the other bands*	**5**: 0°, ±20° and ±58°
Nadir view, at-ground swath width	2663km[@]	1,556 km	100km
Spatial Resolution	1x1km at nadir[@]	5.2km^2, subject to modification	5.4 x 4.6 km[#] for all view angles

*note that the set of viewing angles for HARP2 are slightly different for each spectral channel.
[#]the SPEXone spatial sampling is 2.6km^2.
[@]Since OCI only views at 20˚ forward or aft, the OCI swath width is presented at that angle, and the spatial resolution at those angles are slightly larger. The onboard binning scheme (HARP2) and optical design (SPEXone) minimize footprint growth at larger view angles than nadir for those instruments.

The intent of the L1C format is to represent radiometric data observed by the three PACE instruments on a common grid. For grids with data from multiple instruments, this would facilitate their merged usage in a L1C to L2 algorithm. For example, OCI SWIR channels could provide coarse mode aerosol information for a SPEXone aerosol retrieval and HARP2 multi-angle measurements may complement OCI measurements by providing greater atmospheric information for, e.g. atmospheric correction. Potential uses for such combined datasets were explored by the first PACE Science Team, described in reviews such as Frouin et al., 2019 and Remer et al., 2019. Additionally, a L1C product could aid in easy instrument cross calibration or validation. At least five types of files will be generated, one containing only the L1C grid, one

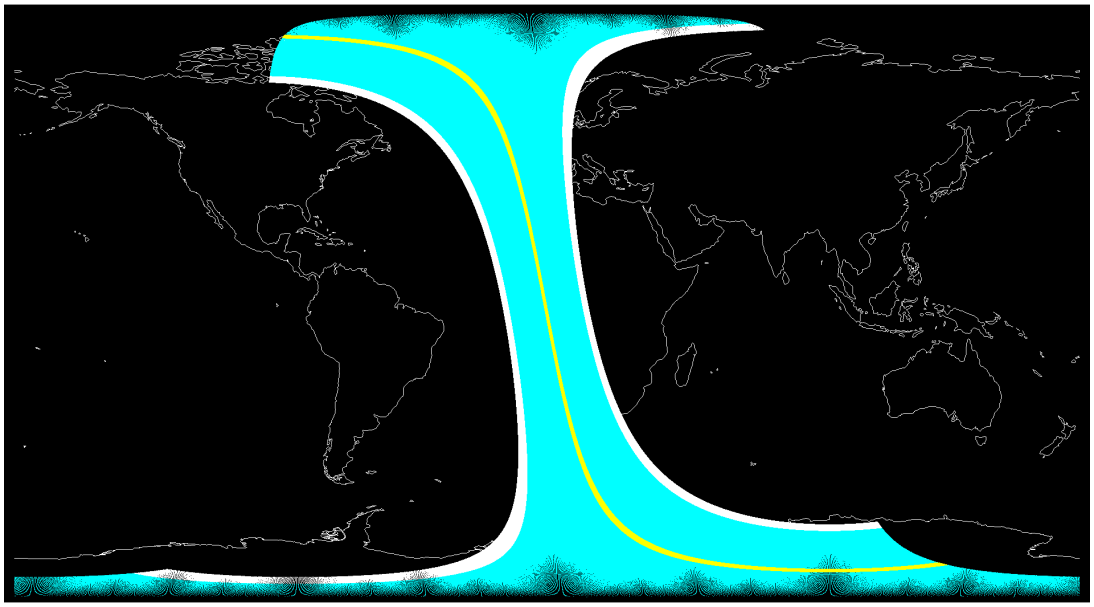

Figure 1 Expected L1C coverage for OCI (white), HARP2 (teal) and SPEXone (yellow).

for each PACE instrument (OCI, HARP2 and SPEXone) and a fourth to contain ancillary data (such as OCI derived cloud flags, and MERRA-2 (Gelaro et al., 2017) reanalysis data). Due to

varying spatial resolution, these files may have different grid sizes, but compatibility will be maintained by constraining these sizes to multiples of each other.

2 FILE NAME CONVENTION

The file naming convention of the Ocean Biology Processing Group (OBPG) and the Ocean Biology Distributed Active Archive Center (OB-DAAC), who will be performing the full L1C data processing and archival, respectively, is described on the OB-DAAC website: https://oceancolor.gsfc.nasa.gov/resources/docs/filenaming-convention/

MMMM_IIII_TTT.YYYYMMDDTHHMMSS.LLLL.PPPP.SSSS.pppp.RRRR.NRT.nc

- MMMM*: variable-length uppercase character string indicating the "mission".
  - e.g. AQUA, PACE, S3A
- IIII: variable-length uppercase character string indicating the instrument
  - e.g. OCI (PACE Ocean Color Instrument)
- YYYYMMDDTHHMMSS: ISO8601 time format, where YYYY is the 4-digit year, MM is the two-digit month, DD is the two-digit day, T indicates the time follows this character, HHMMSS are the two-digit hour, minutes, and seconds, respectively.
- LLLL: variable-length character string indicating the level.
  - e.g. L1B, L2, L3m
- Undefined character sequences noted above may be omitted.

* The mission identifier could be a reasonably shortened representation, e.g. Sentinel-3A = S3A

Unlike the full L1C file template, which applies to the ancillary and observational data files, the L1C grid filename does not include the sensor name. None of the file names will include period indicator, suite identifier, product identifier resolution and near real time identifier described in the file naming convention referenced above.

Example filenames for January 15th, 2023 at 12:34:56 UTC would be:

L1C grid:	PACE_20230115T123456.L1C.nc
OCI:	PACE_OCI.20230115T123456.L1C.nc
HARP2:	PACE_HARP.20230115T123456.L1C.nc
SPEXone:	PACE_SPEX.20230115T123456.L1C.nc
Ancillary:	PACE_ANC.20230115T123456.L1C.nc

Note the PACE_ANC* files will contain ancillary data represented on the L1C grid. This could include assimilated meteorological data, cloud flags, or other external or derived information.

Airborne datasets represented with the L1C file structure described in this document may use a different naming convention than described above. For example, the convention currently in use for the PACE-PAX airborne field campaign at the NASA Langley Suborbital Science Data for Atmospheric Composition archive (https://www-air.larc.nasa.gov/missions/pacepax) is:

MMMM-IIII-LLLL-FFFF_PPPP_YYYYMMDDTHHMMSS_RR.nc

- MMMM*: variable-length uppercase character string indicating the "field campaign".
  - e.g. PACE-PAX

- IIII: variable-length uppercase character string indicating the instrument
    - e.g. OCI (PACE Ocean Color Instrument)
- LLLL: variable-length character string indicating the level.
    - e.g. L1B, L2, L3m
- FFFF: Squared footprint size
    - e.g. 2d6km for 2.6km squared
- PPPP: Aircraft platform
    - e.g. ER2 (ER-2), TO (Twin Otter)
- YYYYMMDDTHHMMSS: ISO8601 time format, where YYYY is the 4-digit year, MM is the two-digit month, DD is the two-digit day, T indicates the time follows this character, HHMMSS are the two-digit hour, minutes, and seconds, respectively.
- RR: Revision number
    - e.g. RA for Revision A

An example is:
PACEPAX-AirSPEX-L1C-2d6km_ER2_20230115123456_RA.nc

3 PROJECTION

The L1C format will use a swath-based Spacecraft Oblique Cylindrical Equal Area (SOCEA) projection (see Snyder, 1978 and 1987 for a description of the Oblique Cylindrical Equal Area projection). This projection will have the vertical centerline aligned with the subsatellite track, horizontal bin spacing representing equal distances transverse to the orbit track, and vertical spacing that preserves the equal area grid. Bins are indexed by row and column, and constructed so that the intersection of the ground track with the equator corresponds to the meeting point of four bins along the centerline of the projection. Note that this projection is similar, but not the same, as the L1C format specified for the forthcoming EUMETSAT Metop-SG A Multi-viewing, Multi-channel and Multi-polarization Imager (3MI) instrument (Lang et al, 2019).

Figure 2 shows a map of the SOCEA projection. A new projection is defined for each orbit, centered about the orbit path, which for the purposes of demonstration is the Prime Meridian in this figure.

Bin size uniformity is an important aspect of the L1C format projection. Ground spatial resolution is generally preserved for the SPEXone instrument, due to narrow swath and specially designed optics for fore and aft views intended for this purpose. This will not be the case, however, for OCI and HARP2. For those instruments, the ground spatial resolution will grow as the view zenith angle increases from nadir. This would be a problem for algorithms that utilize multiple views and instruments, as they are (almost universally) built on the assumption that all observations represent the same location. The SOCEA projection satisfies the requirement for equal area bins, the size of which are described in more detail in the next section.

In addition to the advantages described above, the SOCEA projection is easily viewed as stored. However, the specific projection must be defined for each orbit, and there is no inherent relationship between row/column and latitude/longitude, so the latter must also be stored for each bin.

Another advantage of this format is that users of L2 (geophysical) data are more likely to use a format which can be easily viewed as images, and it is simplest to maintain the projection and format in the L1C to L2 processing. However, we should note the Level 3 binned products will likely use an integer sinusoidal binning scheme (see: https://oceancolor.gsfc.nasa.gov/docs/format/l3bins/)

Figure 2 SOCEA Projection for an orbit track along the Prime Meridian. Cropped from: https://www.giss.nasa.gov/tools/gprojector/help/projections/

4 SPATIAL RESOLUTION AND SWATH

We intend to bin all three instruments to 5.2 x 5.2km horizontal spatial resolution at the surface. This means that the number of bins in the across swath direction will be roughly 519 for OCI, 29 for SPEXone and 457 for HARP2. Data from the full swath for all instruments will be incorporated into the L1C format, including portions of the HARP2 swath that may not have nadir views due to broadening at the most forward and aft viewing angles.

The choice of the use of variable spatial resolutions is a tradeoff. On one hand, we would like to easily match coincident measurements from multiple instruments. On the other, we don't want to degrade an individual instrument's spatial resolution unnecessarily. We have therefore chosen a format that matches the geographic coordinates of the different instruments to a common grid, although in some cases the spacing of that grid for one instrument might be multiples of that of that for another. To assist the usage of multiple instrument datasets simultaneously, the *nadir_bin* field is included that identifies the bin closest to nadir in each swath. Since the subsatellite track forms the boundary between two bins, the bin immediately to the east of this is what is identified by the *nadir_bin* field. Additionally, a tool will be provided that can downsample and/or align data from multiple instruments to the same spatial resolution (see Section 7).

The L1C grid file is based on daytime swath derived from the OCI sensor. The processing code also allows for smaller common grids based on across track bins of SPEXone and HARP2. The L1C files (full or grid) are produced with orbital information extracted from HKT (housekeeping telemetry). L1C files are created as granules with a default size of 5-minutes and swaths (i.e., daytime orbit with up to 10 granules).

5 MULTI-VIEW AGGREGATION

The MAP instruments are designed to capture the angular dependence of scattering for a surface or volume of the atmosphere, which contains additional optical property information. L1C to L2

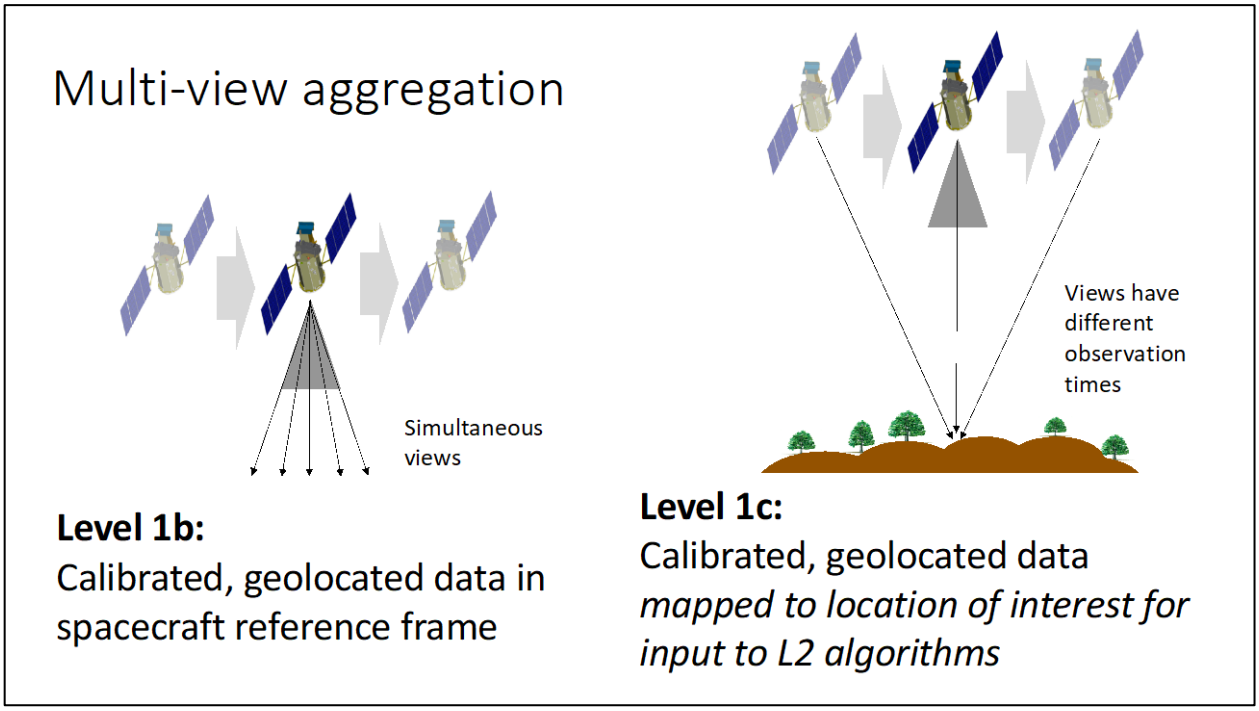

Figure 3 Illustration of multi-view aggregation

algorithms that utilize this information need the data organized so that it represents scattering about a single point. In practice, the multiple angle views are made as the spacecraft flies over that point, so the individual views have different sampling times. This means that the data are organized in a L1B file in a manner that represents multi-angle views at the spacecraft altitude, not the geophysical point of interest. Thus, multi-angle views must be 'aggregated' to a specific ground location. Projection, as is described in Section 2, will achieve this purpose. It is a process that requires knowledge of the height of the bin location. Over the ocean, this height will by default be the ellipsoid surface. Over land, data will be aggregated to the height of a digital elevation model (DEM) at that location. Details of the specific DEM will be included in the file attributes, while the variability of elevations within a specific grid box will be stored in a data field. Currently, the DEM planned for use by PACE is the GEBCO_2019 dataset (https://www.gebco.net/data_and_products/gridded_bathymetry_data/gebco_2019/gebco_2019_info.html, doi:10.5285/836f016a-33be-6ddc-e053-6c86abc0788e), with minor modifications to report the height of a water body surface (not its bathymetry). Retrievals of cloud optical properties (or aerosols above clouds) will require re-aggregation to an alternative height. The L1C product produced for PACE will by default be the surface as described above, however, a software tool to re-aggregate to a given height will also be made available (see Section 7).
We note that multi-angle observations inherently contain information about feature height via parallax, and this can be used to determine cloud top (Moroney et al, 2002), cloud base (Böhm et al, 2019), aerosol plume altitude and wind speed (e.g. Nelson et al., 2013) or multiple cloud layers (Sinclair et al., 2017). Application of these techniques, if performed for PACE, will be a separate process than the L1B to L1C technique we describe here, but may inform the height used in a re-aggregation.

6 DATA FIELDS

The data fields for the L1C format are common for all instruments, although the dimensions may vary. Data are to be organized into four groups:

1. *sensor_views_bands*: contains information on viewing geometry, band center wavelengths and other information common to all bins,
2. *bin_attributes*: contains information specific to each bin,
3. *geolocation_data*: contains latitude, longitude, altitude, observation and solar geometry,
4. *observation_data*: contains the data observed by the instrument.

These data groups will utilize five different dimensions, whose values will be different for each instrument. Table 2 is a description of these dimensions and potential values for each instrument

Table 2 Data dimensions for each instrument.

Dimension	OCI	HARP2	SPEXone
number_of_views	2[a]	90[b]	5
intensity_bands_per_view	286	1	400
polarization_bands_per_view	0	1	50
bins_along_track	4000	4000	4000
bins_across_track	519	457	29

Color is intended to aid cross reference to the data groups tables.

[a] OCI has a 20˚ fore or aft tilt depending on spacecraft hemisphere

[b] HARP2 will have 60 view angles for the channel centered at 669nm, 10 angles otherwise. Each channel will access unique viewing angles so all are indexed independently here.

We are following CF metadata conventions throughout this format (see cfconventions.org) as much as possible within the OBPG framework. The specific CF convention in use is noted as a global attribute

Table 3 contains global attributes that are required for the L1C format.

Table 3 Global attributes

Field	Description
title	PACE [OCI/HARP/SPEX/ANC] Level-1c data
instrument	[OCI/HARP/SPEX/ANC]
conventions	CF-1.8 ACDD-1.3
institution	NASA Goddard Space Flight Center, Ocean Biology Processing Group
license	http://science.nasa.gov/earth-science/earth-science-data/data-information-policy/
naming_authority	gov.nasa.gsfc.sci.oceancolor
keywords_vocabulary	NASA Global Change Master Directory (GCMD) Science Keywords
standard_name_vocabulary	NetCDF Climate and Forecast (CF) Metadata Convention
creator_name	NASA/GSFC
creator_email	data@oceancolor.gsfc.nasa.gov
creator_url	http://oceancolor.gsfc.nasa.gov
project	PACE Project
publisher_name	NASA/GSFC
publisher_email	data@oceancolor.gsfc.nasa.gov
publisher_url	http://oceancolor.gsfc.nasa.gov
processing_level	L1C
cdm_data_type	One orbit swath or granule
history	l1cgen par=PACE_OCI.20220321T201906.L1B.nc.par ofile=PACE_OCI.20220321T201906.L1C.nc outlist=l1c.tmp
cdl_version_date	2021-09-10
product_name	PACE_[OCI/HARP/SPEX/ANC].20230115T123456.L1C..nc
date_created	yyyy-mm-ddThh:mm:ss.sssZ
sun_earth_distance	0.990849042172323 (in AU)
terrain_data_source	Source of terrain data used for aggregation

spectral_response_function	Points to documentation containing this information
systematic_uncertainty_model	Points to documentation with models (equations) for systematic uncertainty for I, DoLP, Q, U or q,u as relevant
nadir_bin	Cross track bin with view zenith angle closest to nadir. Since true nadir is mapped to the sun satellite track which forms a grid edge, this bin is the closest to the right (east) of that. All arrays use 0-base indicies.
bin_size_at_nadir	Bin width/length at nadir. This is a defined parameter size, independent of pixel size.
processing_version	5.31 6/6/2023
startdirection	Ascending
enddirection	Ascending
time_coverage_start	yyyy-mm-ddThh:mm:ss.sssZ
time_coverage_end	yyyy-mm-ddThh:mm:ss.sssZ
geospatial_bounds	Describes the data's 2D or 3D geospatial extent in OGC's Well-Known Text (WKT) Geometry format (reference the OGC Simple Feature Access (SFA) specification). The meaning and order of values for each point's coordinates depends on the coordinate reference system (CRS). The ACDD default is 2D geometry in the EPSG:4326 coordinate reference system. The default may be overridden with geospatial_bounds_crs and geospatial_bounds_vertical_crs (see those attributes). EPSG:4326 coordinate values are latitude (decimal degrees_north) and longitude (decimal degrees_east), in that order. Longitude values in the default case are limited to the [-180, 180) range. Example: 'POLYGON ((40.26 -111.29, 41.26 -111.29, 41.26 -110.29, 40.26 -110.29, 40.26 -111.29))'.
geospatial_bounds_crs	The coordinate reference system (CRS) of the point coordinates in the geospatial_bounds attribute. This CRS may be 2-dimensional or 3-dimensional, but together with geospatial_bounds_vertical_crs, if that attribute is supplied, must match the dimensionality, order, and meaning of point coordinate values in the geospatial_bounds attribute. If geospatial_bounds_vertical_crs is also present then this attribute must only specify a 2D CRS. EPSG CRSs are strongly recommended. If this attribute is not specified, the CRS is assumed to be EPSG:4326. Examples: 'EPSG:4979' (the 3D WGS84 CRS), 'EPSG:4047'.
geospatial_lat_min	Describes a simple lower latitude limit; may be part of a 2- or 3-dimensional bounding region. Geospatial_lat_min specifies the southernmost latitude covered by the dataset.
geospatial_lat_max	Describes a simple upper latitude limit; may be part of a 2- or 3-dimensional bounding region. Geospatial_lat_max specifies the northernmost latitude covered by the dataset.
geospatial_lon_min	Describes a simple longitude limit; may be part of a 2- or 3-dimensional bounding region. geospatial_lon_min specifies the westernmost longitude covered by the dataset. See also geospatial_lon_max.
geospatial_lon_max	Describes a simple longitude limit; may be part of a 2- or 3-dimensional bounding region. geospatial_lon_max specifies the easternmost longitude covered by the dataset. Cases where geospatial_lon_min is greater than geospatial_lon_max indicate the bounding box extends from geospatial_lon_max, through the longitude range discontinuity meridian (either the antimeridian for -180:180 values, or Prime Meridian for 0:360 values), to geospatial_lon_min; for example, geospatial_lon_min=170 and geospatial_lon_max=-175 incorporates 15 degrees of longitude (ranges 170 to 180 and -180 to -175).

The ‘history’ global attribute refers to the command line parameters used to run l1cgen, the OCSSW processing software for deriving L1C products.

Note that fields beginning *geospatial_* follow the conventions of the Earth Science Information Partners (ESIP): https://wiki.esipfed.org/

Table 4 lists the seven fields in the *sensor_views_bands* group. This group defines the specific viewing angles (specified at ground), band center wavelengths and bandpasses (Full width, half maximum, FWHM), and the bandpass integrated, annual average, solar irradiance (F_0) used to calculate radiometric properties.

Table 4 *sensor_views_bands* group

Name	Dimension	Dimension	Unit	Description
sensor_view_angle	number_of_views	-	degrees	Along-track view zenith angles for sensor, at sensor*
intensity_wavelength	number_of_views	intensity_bands_per_view	nm	Intensity field center wavelengths at each view
intensity_bandpass	number_of_views	intensity_bands_per_view	nm	Intensity field bandpasses at each view, defined as Full Width Half Maximum (FWHM).
polarization_wavelength^	number_of_views	polarization_bands_per_view	nm	Polarization field center wavelengths at each view.
polarization_bandpass^	number_of_views	polarization_bands_per_view	nm	Polarization field bandpasses at each view.
intensity_f0#	number_of_views	intensity_bands_per_view	$W\ m^{-2}\ \mu m^{-1}$	Spectral response function convolved mean solar flux at each intensity band and view.

polarization_f0#^	number_of_views	polarization_bands_per_view	W m^{-2} μm^{-1}	Spectral response function convolved mean solar flux at each polarization band and view.

***sensor_view_angle* is defined at the sensor, as it provides a swath independent value at top of atmosphere. Definition of view zenith and azimuth angles at the ground, which depend upon bin location and *sensor_view_angle*, are contained in the *sensor_zenith* and *sensor_azimuth* fields described in the *geolocation_data* group.**

#Spectral function weighted F0 values may require specification individually for different views, as the spectral response functions for those views may vary. If this is not the case for all instruments, these fields will revert to attributes.

^polarization specific fields will only exist for instruments that have polarization sensitivity, ie HARP2 and SPEXone, but not OCI

Table 5 contains the characteristics of two fields within the *bin_attributes* group. This group defines the time at which the spacecraft subsatellite point passes over the across track line, and the offsets from that time for all view angles.

Table 5 *bin_attributes* group

Name	Dimension	Dimension	Dimension	Unit	Description
nadir_view_time*	bins_along_track	-	-	Seconds from UTC midnight	Time nadir view was observed
view_time_offset	bins_along_track	bins_across_track	number_of_views	Seconds	Offset of view angle time to nadir view time

*only this variable appears in bin_attributes group of L1C grid files.

The view_time_offset is defined as: time_gd -mean scantime where time_gd is nadir time at the center of the L1C grid cell and scantime is the scaline time of the sensor computed as arithmetic average for each L1C grid cell. Time offset is positive for the aft views and negative for the forward views.

Table 6 describes the *geolocation_data* group, containing bin coordinates, height (to which the data have been aggregated) and the solar and sensor geometries. Most conventions are described in Patt and Gregg, (1994). The scattering angle, which is the angle from the solar illumination vector at the bin location to the vector in the direction of the sensor view, is also provided. While *scattering_angle* is redundant with other geometry angles, this parameter is included in the L1C file format definition for consistency and ease of use. It is defined:

$$\begin{gathered}\cos\alpha = uu_s + (1-u^2)^{1/2}(1-u_s^2)^{1/2}\cos(\phi + 180^\circ - \phi_s) \\ = -\sin(\theta)\sin(\theta_s)\cos(\phi - \phi_s) - \cos(\theta)\cos(\theta_s) \\ u = \cos(\theta + 180^\circ) \\ u_s = \cos\theta_s\end{gathered} \tag{1}$$

which uses the convention of equation 3.17 in Hansen and Travis, 1974 in the first line but accounts for the definition of geometry that we use (hence the 180˚ shift for sensor zenith and azimuth angles). The second, equivalent, formulation in this equation follows the convention of Gordon and Wang, 1994. An additional earlier work defining the scattering angle is Hovenier, 1969. In equation (1), α is the scattering angle, θ and θ_s are the sensor and solar zenith angles, respectively, and ϕ and ϕ_s are the sensor and solar azimuth angles, respectively

(*sensor_azimuth, solar_azimuth*). Note that 180˚ must be added to *sensor_zenith* and *sensor_azimuth* to align geometry conventions of this document with that of Hansen and Travis, 1974, which considers zenith associated with an upward vector to have a negative sign, and because the associated azimuth angle is rotated 180˚. In this convention, scattering angles of 0˚ and 180˚ are therefore the forward and backscattered directions, respectively.Figure 4 is a schematic of the geometry conventions. The final parameter in this group, *rotation_angle*, is defined in equation 5 below.

Table 7 contains the *observation_data* group. As the name suggests, this group contains the core data fields, which also have the largest dimensionality (4D). The L1C file is to contain data from instruments with sensitivity to linear polarization, which we represent with the Stokes vector:

$$\boldsymbol{I} = \begin{bmatrix} I = \langle E_l E_l^* + E_r E_r^* \rangle \\ Q = \langle E_l E_l^* - E_r E_r^* \rangle \\ U = \langle E_l E_r^* + E_r E_l^* \rangle \\ V = i\langle E_l E_r^* - E_r E_l^* \rangle \end{bmatrix}. \tag{1}$$

Here, the brackets indicate phase average and the * the complex conjugate of an electric field represented by a pair of mutually perpendicular oscillating components, E_l and E_r :

$$E_l = a_l e^{i(\omega t - kz - \varepsilon_l)}$$
$$E_r = a_r e^{i(\omega t - kz - \varepsilon_r)} \tag{2}$$

These components are each associated with unit vectors ***r*** and ***l*** (whose cross product is the propagation direction, *z* is distance in this direction), and where *k* is the wave number, *t* is time, ω is frequency, a_l and a_r are wave amplitudes, and ε_l and ε_r are phases (Hansen et al., 1974).

In a practical sense, the *I* component of the Stokes vector represents the total intensity (a term we use loosely without defining units), while *Q* and *U* contain information about the direction and magnitude of linear polarization. Circular polarization is expressed with *V*, which is henceforth omitted because no PACE instruments are sensitive to this aspect of polarization.

Equations (1) and (2) show that *Q* and *U* are defined with respect to a reference plane, which for the L1C file is defined to be in the local view meridional plane, containing vectors from the observed location to the sensor, and the zenith vector from the observed location. Figure 4 illustrates this and other geometry conventions used in the L1C format.

Some data users may prefer to use Q and U expressed in another plane, such as the scattering plane. Hovenier and van der Mee (1983) and Hovenier (1969) describe the calculations required to convert *Q* and *U* to other reference planes. This uses a rotation matrix, such that:

$$\boldsymbol{I}' = \boldsymbol{L}(\sigma)\boldsymbol{I} \tag{3}$$

where ***I'*** is the Stokes vector represented in the solar scattering plane containing unit vectors of the solar illumination direction (θ_s and ϕ_s) and observation viewing direction (θ and ϕ).

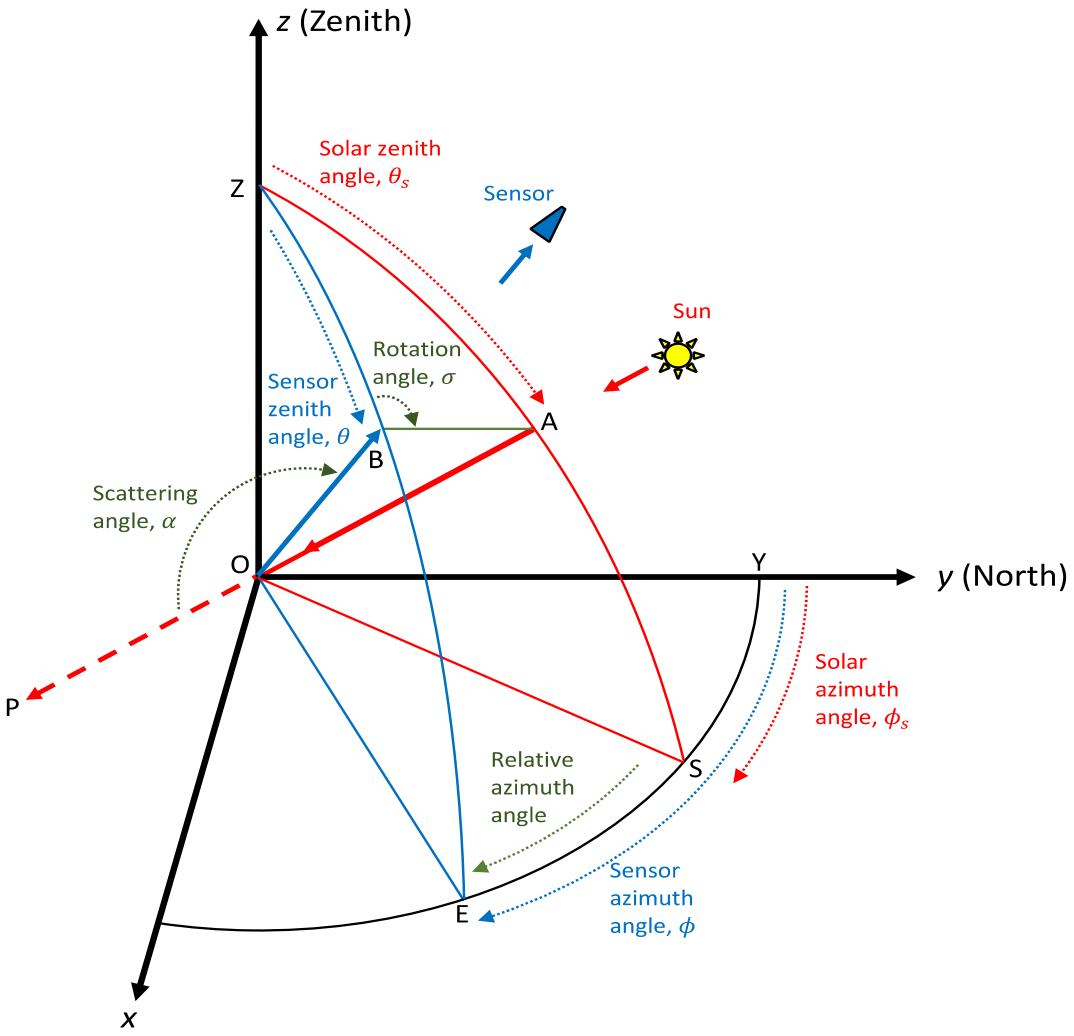

Figure 4 Observation and geometry illustration. The sun illuminates a point at location **O** along the vector **AO**. The associated *solar zenith angle* (θ_s) is the angle **ZOA** from the zenith direction (normal to surface plane) from **O** to the vector in the direction of illumination, **OA**. The *solar azimuth angle* (ϕ_s) is the angle **YOS** due North from **O** to the projection of the Sun vector on the surface plane. The *solar meridional plane* contains vectors **OA** and **OZ** and is illustrated in red in the figure. The sensor observes scattered radiation from a point at location **O** along the vector **OB**. The associated *sensor zenith angle* (θ) is the angle **ZOB** from the zenith direction (normal to surface plane) from **O** to the scattered vector **OB**. The *sensor azimuth angle* (ϕ) is the angle **YOE** due North from **O** to the projection of the sensor observation vector on the surface plane. The *sensor meridional plane* contains vectors **OB** and **OZ** and is illustrated in blue in the figure. Items labeled in green indicate properties relating these two planes. The *scattering angle* (α) is the angle from the solar illumination vector **AOP** to the scattered vector **OB**. The *rotation angle* (σ) is the angle from the *sensor meridional plane* to the *scattering plane* containing the vectors **OB** and **OA**. Finally, the *relative azimuth angle* is the ϕ - ϕ_s difference between the *sensor azimuth angle* and the *solar azimuth angle*. After Hovenier and van der Mee (1983) and Xu and Wang (2019).

The rotation matrix, $\boldsymbol{L}(\sigma)$, is:

$$\boldsymbol{L}(-\sigma) = \begin{bmatrix} 1 & 0 & 0 & 0 \\ 0 & \cos 2\sigma & -\sin 2\sigma & 0 \\ 0 & \sin 2\sigma & \cos 2\sigma & 0 \\ 0 & 0 & 0 & 1 \end{bmatrix} \tag{4}$$

where σ is the angle to rotate from the meridional plane to the scattering plane. Following Hovenier, 1969, it is calculated:

$$\cos\sigma = \frac{-u_s + u\cos\alpha}{\pm(1-\cos^2\alpha)^{1/2}(1-u^2)^{1/2}}$$

$$= \frac{-u_s + u\cos\alpha}{\frac{|\sin(\phi-\phi_s)|}{\sin(\phi-\phi_s)}\sin(\alpha)(1-u^2)^{1/2}}$$

$$= \tan^{-1}\frac{\mathbf{OB}\cdot(\mathbf{OZ}\times\mathbf{OA})}{(\mathbf{OZ}\cdot\mathbf{OA})-(\mathbf{OB}\cdot\mathbf{OA})(\mathbf{OB}\cdot\mathbf{OZ})} \quad (5)^1$$

where the denominator is positive if $0° < \phi - \phi_s < 180°$ and negative if $-180° < \phi - \phi_s < 0°$. An alternative which does not require this logical assessment and is valid for all $\phi - \phi_s$ is written in the second line of the equation. The third line is expressed in vector form as in Wertz 1978, Appendix C, which calculates the rotation from **OZ** to **OA** about **OB** in Figure 4. In this equation, the numerator is proportional to sin(σ) and the denominator to cos(σ), with the proportionality constant being the same for both. Note that the form of the arctangent with two arguments provides a result in the range +/-π.

The rotation angle, σ, is provided in the *geolocation_data* group as the *rotation_angle* field. Calculation of the Stokes vector rotated into the scattering plane from the meridional plane is performed with:

$$\boldsymbol{I}' = \begin{bmatrix} I \\ \mathrm{Q}\cos 2\sigma + U\sin 2\sigma \\ -Q\sin 2\sigma + U\cos 2\sigma \end{bmatrix} \tag{6}$$

Note that I is unchanged with rotation, and we have omitted V as it is not measured by PACE sensors.

[1] Another method is to calculate the scattering angle as $\cos\alpha = \cos\theta\cos\theta_s + |\sin\theta\sin\theta_s|\cos(\phi-\phi_s)$ and the rotation angle as $\cos\sigma = \frac{-\cos\theta_s + \cos\theta\cos\alpha}{\sin\alpha|\sin\theta|}$. If $\phi - \phi_s > \pi$ or $\theta - \theta_s > \pi$ then set $\sigma = -\sigma$.

Table 6 *geolocation_data* group.

Variable name	Dimension	Dimension	Dimension	Unit	Description
latitude**	bins_along_track	bins_across_track	-	Degrees North	Latitude of bin location
longitude**	bins_along_track	bins_across_track	-	Degrees East	Longitude of bin location
height**	bins_along_track	bins_across_track	-	Meters	(aggregation) height of bin location above the ellipsoid.
height_stdev	bins_along_track	bins_across_track	-	Meters	Standard deviation of terrain altitude within bin
sensor_azimuth_angle	bins_along_track	bins_across_track	number_of_views	Degrees from North	ϕ: Azimuth angle from the bin location to the sensor, defined clockwise from north.*
sensor_zenith_angle	bins_along_track	bins_across_track	number_of_views	Degrees	θ: Zenith angle from the bin location to the sensor, defined with respect to the zenith pointing vector.*
solar_azimuth_angle	bins_along_track	bins_across_track	number_of_views	Degrees from North	ϕ_s: Azimuth angle from the bin location to the sun, defined clockwise from north.*
solar_zenith_angle	bins_along_track	bins_across_track	number_of_views	Degrees	θ_s: Zenith angle from the bin location to the sun, defined with respect to the zenith pointing vector.*
scattering_angle	bins_along_track	bins_across_track	number_of_views	Degrees	α: Angle from the sun illumination vector to the vector in the direction of the sensor.#
rotation_angle	bins_along_track	bins_across_track	number_of_views	Degrees	σ: Angle to rotate polarization reference frame from meridional plane to solar scattering plane.

*** we follow the geometry conventions of the PACE SDPS, as described in Patt and Gregg, 1994. Range of these values is 0° to 360° for azimuth angles, and 0° to 90° for zenith angles.**
 # CF convention is to use units of radians for this field, but to be consistent with other geometries, we use degrees.
****only these variables appear in the geolocation_data group of L1C grid files.**

To avoid the complication of reference frame and compress Q and U into one parameter, a commonly used polarimetric quantity is the Degree of Linear Polarization (DoLP):

$$DoLP = \frac{\sqrt{Q^2 + U^2}}{I} \tag{7}$$

which has the benefit of condensing Q and U into a single, reference plane insensitive, parameter. While this does represent a loss of information, in many observation systems (including the PACE MAPS) some systematic uncertainties cancel when represented by DoLP, leading to low relative uncertainty. Assessment of the polarization angle can be represented by the Angle of Linear Polarization (AoLP):

$$AoLP = \frac{1}{2}\tan^{-1}\frac{U}{Q} \tag{8}$$

where we adopt the common convention (Hansen and Travis, 1974) to select the value in the interval $0 \leq \text{AoLP} \leq \pi$ for which cos(2AoLP) has the same sign as Q.

An alternative Q and U formulation, which takes advantage of normalization with respect to I, but preserves the sign and direction in Q and U, is:

$$q = \frac{Q}{I}; u = \frac{U}{I} \tag{9}$$

This is expressed as *q_over_i* and *u_over_i* in the *observation_data* group, as field names are case insensitive.

Depending on the application, L1C to L2 algorithms may have a preference for one or another representation of the polarimetric state. Furthermore, different instruments may vary in the inherent polarimetric measurement that is made. In our case, HARP2 data are produced as Q and U, while for SPEXone it is q and u. Furthermore, the spectral sampling (and resolution) for SPEXone varies for I, q and u (see Table 1; I has higher spectral resolution than q and u). Conversion of SPEXone q and u to Q and U or *DoLP,* therefore, requires using I that has been spectrally sampled like q and u, which we call *i_polsample*.

Table 7 *observation_data* group

Name	Dimension	Dimension	Dimension	Dimension	Unit	Description
number_of_observations	bins_along_track	bins_across_track	number_of_views	-	Unitless	Observations contributing to bin from each view
qc	bins_along_track	bins_across_track	number_of_views	intensity_bands_per_view	Unitless	Quality indicator
i	bins_along_track	bins_across_track	number_of_views	intensity_bands_per_view	W m^{-2} sr^{-1} μm^{-1}	I Stokes vector component
i_stdev	bins_along_track	bins_across_track	number_of_views	intensity_bands_per_view	W m^{-2} sr^{-1} μm^{-1}	Standard deviation of I in bin
qc_polsample	bins_along_track	bins_across_track	number_of_views	polarization_bands_per_view	Unitless	Quality indicator
i_polsample	bins_along_track	bins_across_track	number_of_views	polarization_bands_per_view	W m^{-2} sr^{-1} μm^{-1}	I Stokes vector component at polarimeter spectral sampling
i_polsample_stdev	bins_along_track	bins_across_track	number_of_views	polarization_bands_per_view	W m^{-2} sr^{-1} μm^{-1}	Standard deviation of I_POLSAMPLE in bin
q	bins_along_track	bins_across_track	number_of_views	polarization_bands_per_view	W m^{-2} sr^{-1} μm^{-1}	Q Stokes vector component
q_stdev	bins_along_track	bins_across_track	number_of_views	polarization_bands_per_view	W m^{-2} sr^{-1} μm^{-1}	Standard deviation of Q in bin
u	bins_along_track	bins_across_track	number_of_views	polarization_bands_per_view	W m^{-2} sr^{-1} μm^{-1}	U Stokes vector component
u_stdev	bins_along_track	bins_across_track	number_of_views	polarization_bands_per_view	W m^{-2} sr^{-1} μm^{-1}	Standard deviation of U in bin
q_over_i	bins_along_track	bins_across_track	number_of_views	polarization_bands_per_view	Unitless	Q over I (little q) Stokes vector component
q_over_i_stdev	bins_along_track	bins_across_track	number_of_views	polarization_bands_per_view	Unitless	Standard deviation of Q_OVER_I in bin

u_over_i	bins_along_track	bins_across_track	number_of_views	polarization_bands_per_view	Unitless	U over I (little u) Stokes vector component
u_over_i_stdev	bins_along_track	bins_across_track	number_of_views	polarization_bands_per_view	Unitless	Standard deviation of U_OVER_I in bin
dolp	bins_along_track	bins_across_track	number_of_views	polarization_bands_per_view	Unitless	Degree of linear polarization (DOLP)
dolp_stdev	bins_along_track	bins_across_track	number_of_views	polarization_bands_per_view	Unitless	Standard deviation of DOLP in bin
aolp	bins_along_track	bins_across_track	number_of_views	polarization_bands_per_view	degrees	Angle of linear polarization (AOLP)
aolp_stdev	bins_along_track	bins_across_track	number_of_views	polarization_bands_per_view	degrees	Standard deviation of AOLP in bin

To balance the competing desire to contain polarimetric data as measured, provide for an accurate conversion to the variety of polarimetric forms that might be used in an algorithm and do so in as compact a manner possible, we intend to fill fields in Table 7 differently for each instrument, as follows:

OCI: *i*

HARP2: *i; q; u*

SPEXone: *i; i_polsample; q_over_i; u_over_i*

Redundant but convenient: *dolp, aolp*

In this way, HARP2 data can be easily converted to *q* and *u* using equation (5). SPEXone data can be converted to *Q* and *U* by inverting equation (5) and using *i_polsample* (*I* resampled on the *q* and *u* spectral sensitivity).

Measurement uncertainty can be quite variable for polarization, and also different than for *I*. Algorithms that utilize polarimetric data need (unique) measurement uncertainty estimates to properly weight the different types of data that are used. Therefore, the *_variability* fields are used to represent the square of the standard deviation of the binned data (sigma squared), which is representative of random errors. There would be combined (added in quadrature, presumably) with estimates of systematic uncertainty noted in the *systematic_uncertainty_model* attribute (see Knobelspiesse et al., 2019 for examples of uncertainty models for MAPs).

I, Q, and *U* have units of radiance, (W sr^{-1} m^{-2} per μm). Conversion to (unitless) reflectance is performed by calculating

$$R_{[I,Q,U]} = \frac{[I,Q,U]\pi r^2}{F_0 \cos\theta_s} \tag{10}$$

Where *r* is the sun earth distance relative to the distance at which F_0 is defined (in *sun_earth_distance* global attribute), F_0 is the mean solar flux in W/m^2 (*intensity_f0* or *polarization_f0*), and θ_s is the solar zenith angle (*solar_zenith_angle*).

7 EXTERNAL DATA AND SOFTWARE

Withing the PACE SDS, the L1C format is implemented with the *l1cgen* software module within OCSSW. This module will have several processing modes that will be described in the OCSSW documentation. Some of the modes will perform the following:

Altitude re-aggregation
A software tool will be provided that can be used to re-aggregate the data to a different height, and provide a modified L1C product representative of that height. The default aggregation height in L1C files is the surface, as specified by the terrain height on land and the ellipsoid over the ocean. This tool will take L1B files as input.

Ancillary and L2 data on the L1C grid
Some L1C to L2 algorithms will require either derived or ancillary data on the L1C grid. Those data will be kept in a separate file (L1C-ancillary) which has the same *geolocation_data* group as the L1C files, but a different *observation_data* group that could, for example, contain L2 products represented on the L1C grid, such as:

1. OCI derived cloud fraction
2. OCI derived cloud phase
3. OCI derived cloud top height
4. [SOME OTHER ALGORITHM] derived cloud top height
5. [SOME ALGORITHM] derived aerosol layer height
6. OCI derived Cloud Effective Radius
7. Ancillary data from MERRA: O3 profile, NO2 profile, temperature profile, pressure profile, relative (or specific) humidity profile.

8 AIRBORNE DATASETS

This format can also be a guide for representation of airborne remote sensing datasets such as those that will be produced by the PACE-PAX field campaign. This would not necessarily be geolocated in the same manner as PACE satellite products, but would preserve the group and field naming convention and organization to maximize compatibility with L1C to L2 processing software developed for use for PACE. This will aid validation efforts.

These files will require an additional group, aircraft_platform, to describe aircraft specific quantities. An example group is provided below; data producers may require additional fields. As much as is practical, producers should use the convention provided below and be CF compliant.

Table 8 *aircraft_platform* group

Name	Dimension	Unit	Description
gps_time	bins_along_track	s	GPS time of instant of the data acquisition
gps_quality	bins_along_track	1	Quality of GPS signal indicator
platform_asl	bins_along_track	m	Platform GPS altitude in ASL
platform_lat	bins_along_track	degrees	Platform GPS latitude
platform_lon	bins_along_track	degrees	Platform GPS longitude
platform_heading	bins_along_track	deg	Platform heading angle

platform_tracking	bins_along_track	deg	Platform tracking angle
platform_pitch	bins_along_track	deg	Platform pitch angle
platform_roll	bins_along_track	deg	Platform roll angle
platform_yaw	bins_along_track	deg	Platform yaw angle
platform_trueairspeed	bins_along_track	m.s-1	Platform true air speed
platform_groundspeed	bins_along_track	m.s-1	Platform ground speed
static_temperature	bins_along_track	degC	static air temperature at platform location
static_pressure	bins_along_track	hPa	Static air pressure at platform location
wingflex	bins_along_track	deg	Applied wingflex correction, if relevant

All data variables in the *aircraft_platform* group should have "long_name" and "units" attributes. If missing data flags (e.g., NaN) or fill values are used, these variables should have "missing_value" or "_FillValue" attribute.

9 REFERENCES

Böhm, C., Sourdeval, O., Mülmenstädt, J., Quaas, J., and Crewell, S., 2019. Cloud base height retrieval from multi-angle satellite data, *Atmos. Meas. Tech.,* 12, 1841–1860, https://doi.org/10.5194/amt-12-1841-2019.

Frouin, R. J., B. A. Franz, A. Ibrahim, K. Knobelspiesse, Z. Ahmad, B. Cairns, J. Chowdhary, H. M. Dierssen, J. Tan, O. Dubovik, X. Huang, A. B. Davis, O. Kalashnikova, D. R. Thompson, L. A. Remer, E. Boss, O. Coddington, P.-Y. Deschamps, B.-C. Gao, L. Gross, O. Hasekamp, A. Omar, B. Pelletier, D. Ramon, F. Steinmetz, and P.-W. Zhai. 2019. Atmospheric Correction of Satellite Ocean-Color Imagery During the PACE Era. *Frontiers in Earth Science*, 7: [10.3389/feart.2019.00145]

Gelaro, R., McCarty, W., Suárez, M. J., Todling, R., Molod, A., Takacs, L., Randles, C. A., Darmenov, A., Bosilovich, M. G., Reichle, R., and others 2017. The modern-era retrospective analysis for research and applications, version 2 (MERRA-2), *Journal of Climate*, 30(14), 5419--5454.

Gordon, H. R. and Wang, M.: Retrieval of water-leaving radiance and aerosol optical thickness over the oceans with SeaWiFS: a preliminary algorithm, Appl. Optics, 33(3), 443--452 , 1994.

Hansen, J.E. and Travis, L.D., 1974. Light scattering in planetary atmospheres. *Space science reviews*, *16*(4), pp.527-610.

Hasekamp, O.P., Fu, G., Rusli, S.P., Wu, L., Di Noia, A., aan de Brugh, J., Landgraf, J., Smit, J.M., Rietjens, J. and van Amerongen, A., 2019. Aerosol measurements by SPEXone on the NASA PACE mission: expected retrieval capabilities. *Journal of Quantitative Spectroscopy and Radiative Transfer*, *227*, pp.170-184.

Hovenier, J. W.: Symmetry Relationships for Scattering of Polarized Light in a Slab of Randomly Oriented Particles, J. Atmos. Sci., 26(3), 488--499, 1969.

Hovenier, J.W. and Van der Mee, C.V.M., 1983. Fundamental relationships relevant to the transfer of polarized light in a scattering atmosphere. *Astronomy and Astrophysics*, *128*, pp.1-16.

Knobelspiesse, K., Q. Tan, C. Bruegge, B. Cairns, J. Chowdhary, B. van Diedenhoven, D. Diner, R. Ferrare, G. van Harten, V. Jovanovic, M. Ottaviani, J. Redemann, F. Seidel, and K. Sinclair. 2019. Intercomparison of airborne multi-angle polarimeter observations from the Polarimeter Definition Experiment. *Applied Optics*, 58 (3): 650 [10.1364/ao.58.000650]

Lang, R., Poli, G., Fougnie, B., Lacan, A., Marbach, T., Riedi, J., Schlussel, P., Couto, A. and Munro, R., 2019. The 3MI Level-1C geoprojected product–definition and processing description. *Journal of Quantitative Spectroscopy and Radiative Transfer*, *225*, pp.91-109.

Martins, J.V., Fernandez-Borda, R., McBride, B., Remer, L. and Barbosa, H.M., 2018, July. The Harp Hype Ran Gular Imaging Polarimeter and the Need for Small Satellite Payloads with High Science Payoff for Earth Science Remote Sensing. In *IGARSS 2018-2018 IEEE International Geoscience and Remote Sensing Symposium* (pp. 6304-6307). IEEE.

Moroney, C., Davies, R. and Muller, J.P., 2002. Operational retrieval of cloud-top heights using MISR data. *IEEE Transactions on Geoscience and Remote Sensing*, *40*(7), pp.1532-1540.

Nelson, D., Garay, M., Kahn, R. and Dunst, B., 2013. Stereoscopic height and wind retrievals for aerosol plumes with the MISR INteractive eXplorer (MINX). *Remote Sensing*, *5*(9), pp.4593-4628.

Patt, F. S. and Gregg, W. W., 1994. Exact closed-form geolocation algorithm for Earth survey sensors, Int. J. Remote Sens., 15(18), 3719-3734 , https://doi.org/10.1080/01431169408954354, 1994.

Remer, L. A., K. Knobelspiesse, P.-W. Zhai, F. Xu, O. V. Kalashnikova, J. Chowdhary, O. Hasekamp, O. Dubovik, L. Wu, Z. Ahmad, E. Boss, B. Cairns, O. Coddington, A. B. Davis, H. M. Dierssen, D. J. Diner, B. Franz, R. Frouin, B.-C. Gao, A. Ibrahim, R. C. Levy, J. V. Martins, A. H. Omar, and O. Torres. 2019. Retrieving Aerosol Characteristics From the PACE Mission, Part 2: Multi-Angle and Polarimetry. *Frontiers in Environmental Science,* 7: [10.3389/fenvs.2019.00094]

Sinclair, K., B. van Diedenhoven, B. Cairns, J. Yorks, A. Wasilewski, and M. McGill, 2017: Remote sensing of multiple cloud layer heights using multi-angular measurements. *Atmos. Meas. Tech.*, 10, 2361-2375, doi:10.5194/amt-10-2361-2017.

Snyder, J. P. 1978: The space oblique Mercator projection, Photogramm. Eng. Remote Sensing, 44, 585-596, 140.

Snyder, J.P., 1987. *Map projections--A working manual* (Vol. 1395). US Government Printing Office.

Werdell, P. J., M. J. Behrenfeld, P. S. Bontempi, E. Boss, B. Cairns, G. T. Davis, B. A. Franz, U. B. Gliese, E. T. Gorman, O. Hasekamp, K. D. Knobelspiesse, A. Mannino, J. V. Martins, C. R. McClain, G. Meister, and L. A. Remer. 2019. The Plankton, Aerosol, Cloud, ocean Ecosystem (PACE) mission: Status, science, advances. *Bulletin of the American Meteorological Society*, 100 (9): 1775–1794 [10.1175/bams-d-18-0056.1]

Spacecraft Attitude Determination and Control, edited by J. R. Wertz, D. Reidel Publishing Company, Dordrecht, Holland, 1978.

Xu, X. and Wang, J.: UNL-VRTM, A Testbed for Aerosol Remote Sensing: Model Developments and Applications, in: Springer Series in Light Scattering: Volume 4: Light Scattering and Radiative Transfer, edited by: A. Kokhanovsky, Springer International Publishing, Cham, 1--69, https://doi.org/10.1007/978-3-030-20587-4_1, 2019.

10 APPENDIX A: ACRONYMS

3MI	Multi-viewing, Multi-channel and Multi-polarization Imager
AoLP	Angle of Linear Polarization
CDL	Common Data Label
DEM	Digital Elevation Model
DNH	Do-No-Harm
DoLP	Degree of Linear Polarization
ESIP	Earth Science Information Partners (ESIP) https://wiki.esipfed.org/
FWHM	Full width, half maximum
HARP2	Hyper-Angular Rainbow Polarimeter-2
L1C	Level 1c
L2	Level 2
MAP	Multi-angle polarimeter
MISR	Multi-angle Imaging SpectroRadiometer
MODIS	Moderate Resolution Imaging Spectroradiometer
OBPG	Ocean Biology Processing Group
OB.DAAC	Ocean Biology Distributed Active Archive Center
OCI	Ocean Color Instrument
OCSSW	Ocean Color Science Software (https://oceancolor.gsfc.nasa.gov/docs/ocssw/)
PACE	Plankton, Aerosol, Cloud, ocean Ecosystem
SOCEA	Spacecraft Oblique Cylindrical Equal Area
SPEXone	Spectro-Polarimeter for Planetary Exploration-one
TBD	To be determined
TOA	Top of Atmosphere

11 APPENDIX B: EXAMPLE FILES

Simulated datasets in the L1C format have been created for several datasets, which are available from the OB.DAAC at a descriptive page: https://oceancolor.gsfc.nasa.gov/data/pace/test-data/ and via direct access: https://oceandata.sci.gsfc.nasa.gov/directdataaccess/Level-1C/

Previous Volumes in This Series

Volume 1 *April 2018*	ACE Ocean Working Group recommendations and instrument requirements for an advanced ocean ecology mission
Volume 2 *May 2018*	Pre-Aerosol, Clouds, and ocean Ecosystem (PACE) Mission Science Definition Team Report
Volume 3 *October 2018*	Polarimetry in the PACE mission: Science Team consensus document
Volume 4 *October 2018*	Cloud retrievals in the PACE mission: Science Team consensus document
Volume 5 *December 2018*	Mission Formulation Studies
Volume 6 *December 2018*	Data Product Requirements and Error Budgets
Volume 7 *December 2018*	Ocean Color Instrument (OCI) Concept Design Studies
Volume 8 *September 2020*	The PACE Science Data Product Selection Plan
Volume 9 *October 2020*	PACE Application Plan
Volume 10 *March 2022*	ACE Ocean Product Accuracy Assessments: A record of the state of the art circa 2010
Volume 11 *June 2023*	The PACE Postlaunch Airborne eXperiment (PACE-PAX)